Available online at www.sciencedirect.com

SCIENCE DIRECT®

Remote Sensing of Environment 97 (2005) 163 – 173

Remote Sensing of Environment

www.elsevier.com/locate/rse

Using AVIRIS to assess hemlock abundance and early decline in the Catskills, New York

Jennifer Pontius[a,*], Richard Hallett[b], Mary Martin[c]

[a]USDA Forest Service-NRS, 271 Mast Road, Durham, NH 03024, United States
[b]USDA Forest Service-NRS, 271 Mast Road, Durham, NH 03024, United States
[c]Complex Systems Research Center, University of New Hampshire, Morse Hall, Durham, NH 03824, United States

Received 7 October 2004; received in revised form 28 March 2005; accepted 10 April 2005

Abstract

In order to aid land managers in monitoring and controlling the ongoing hemlock woolly adelgid outbreak, more accurate landscape scale tools are required to locate the hemlock resource, identify infestation and spot early decline. To this end, NASA's Airborne Visible Infra-red Imaging Spectrometer was flown over the infestation front in the Catskills region of New York during the summer of 2001. Mixture Tuned Matched Filtering in ENVI was used to "unmix" spectra and quantify the hemlock signature contribution to each pixel. The resulting percent hemlock basal area coverage correctly identified hemlock dominated pixels (>40% basal area) with 83% accuracy. Key wavelengths and health indices were examined to determine if a subset of wavelengths could accurately predict an 11-class decline rating system. A linear regression based on reflectance at a chlorophyll sensitive wavelength (*R*683 nm), coupled with a water band index (*R*970/*R*900), was able to predict decline with 85% accuracy. The extreme accuracy at the low (0–3) end of the range indicated that these wavelengths might be used to assess early decline, before visual symptoms are apparent in the field.

Keywords: Chlorophyll a and b; Hemlock woolly adelgid; Mixture Tuned Matched Filtering; Forest health; Hyperspectral remote sensing

1. Introduction

Over the past century, one of the greatest threats to the health of North American forests has been the introduction of exotic pathogens and insect pests. Such invasions often result in drastic and long-term changes in forest ecosystems, aesthetic conditions and important natural resources (Castello et al., 1995; Liebhold et al., 1995). During the 20th century, widespread mortality and decline has occurred among species such as American chestnut (*Castanea dentate* Marsh), American elm (*Ulmus americana*), oak (*Quercus* spp.) and American beech (*Fagus grandifolia* Ehrh.). Currently, eastern hemlock (*Tsuga canadensis* L. Carr.) forests are threatened by another major forest pest, the hemlock woolly adelgid (*Adelges tsugae* Annand) (HWA).

Since the 1980's when HWA first surfaced in the Northeast, it has spread rapidly, leading to decline and mortality in over eleven states, from North Carolina to Massachusetts (Souto et al., 1995). Although its trajectory is somewhat unpredictable, current estimates are that HWA is spreading 10–15 miles a year into uninfested areas (Orwig & Foster, 1998; Souto et al., 1995). Once settled on young hemlock twigs, HWA causes needle loss, bud mortality and finally branch and tree mortality, typically within 4 to 6 years (McClure, 1991; Shields et al., 1995). Most infested eastern hemlock trees have shown no resistance to HWA and little chance for recovery (McClure, 1995).

The potentially severe consequences and large scale of the HWA infestation requires that land managers be familiar with the actual location of the hemlock resource and its health and infestation status. Most assessments of forest decline involve time-consuming field based methods. Although these methods are valuable in monitoring gross changes over time, they are not able to identify trees in the

* Corresponding author. Tel.: +1 603 868 7739; fax: +1 603 868 7604.
E-mail address: jennifer.pontius@unh.edu (J. Pontius).

0034-4257/$ - see front matter © 2005 Elsevier Inc. All rights reserved.
doi:10.1016/j.rse.2005.04.011

very early stages of decline (Sampson et al., 2000) or assess large acreages. Remote sensing technologies are the most viable option to assist land managers in health assessment and monitoring at a regional scale.

To date, remote sensing of forest health has involved the classification of various degrees of defoliation and mortality using aerial photography or coarse spectral resolution visible/NIR space-based sensors, such as Landsat Thematic Mapper (TM). Lambert et al. (1995) used Landsat-TM imagery to separate three categories of damage in Norway spruce with 75% accuracy. Similar defoliation based studies have predicted four classes of hemlock defoliation with moderate accuracy (Royle & Lathrop, 1997, 2002; Royle et al., 1995).

The use of this type of imagery is limited in several ways. For example, in areas of mixed coniferous vegetation, errors can be introduced due to the spectral similarity between damaged trees of one species to healthy spectra of other species (Rosengren & Ekstrand, 1988). In addition it can be equally difficult to distinguish a severely defoliated hemlock stand from an inherently sparse healthy stand (Royle & Lathrop, 2002). Finally, when decline is measured solely as a function of defoliation, earlier signs such as reductions in photosynthesis and chlorophyll content are not detected. When Landsat-TM data are used to assess forest health, moderate and light damage stands are often difficult to distinguish due to overlap in their reflectance ranges (Lambert et al., 1995; Royle & Lathrop, 2002).

Many studies have demonstrated that hyperspectral instruments are needed to accurately detect detailed changes in vegetation condition (Treitz & Howarth, 1999). Many diagnostic features for estimating plant decline are located in relatively narrow wavebands, interspersed with insensitive features (Treitz & Howarth, 1999). Ratios or pairs of wavelengths (indices) tend to highlight significant features while correcting for geometrical and background effects (Baret & Guyot, 1991) by targeting decline sensitive bands paired with an insensitive "control" band (Treitz & Howarth, 1999). Such simple transformations have been closely correlated with plant characteristics, without the sensitivity to external variables such as sun angle or instrument variability (Pinty et al., 1993).

Common stress responses, such as the "blue shift" away from the normal inflection point of the red edge reflectance feature, are also dependent on the use of hyperspectral instruments to pick up the subtle shifts (on the order of 5 nm) that accompany pre-visual decline (Rock et al., 1988).

Using a 72-channel CASI sensor, Sampson et al. (2000) found strong relationships between reflectance and leaf chlorophyll content. Because chlorophyll content is known to decrease in stressed vegetation, it may be one of the most important indicators of early decline (Zarco-Tejada et al., 2000). Chlorophyll a and b content are particularly good indicators of decline because of their direct role in photosynthesis. Narrow wavebands near 700 nm where changes in chlorophyll absorption are easily detectable have been recommended for early detection of forest damage (Hoque et al., 1990, 1992) and were able to detect decreased vigor, before visual symptoms were apparent, in pine seedling canopies (Cibula & Carter, 1992).

Existing literature and previous work by the authors (Pontius et al., 2005) highlight several indices and wavelengths that are able to identify decline, including pre-visual symptoms, using field and benchtop instruments. This study was designed to expand this laboratory based work to a remote sensing platform. Specifically our aim was to:

1. quantify the ability of AVIRIS to map hemlock abundance,
2. identify potential wavelengths for early hemlock decline detection, and
3. determine if hyperspectral imagery from a remote sensing platform can predict early hemlock decline symptoms.

2. Methods

2.1. Remote sensing data

On July 20, 2001, hyperspectral imagery from NASA's Airborne Visible/Infrared Imaging Spectrometer (AVIRIS) was obtained for the 700,000 acre Catskills State Park region. Flown on an ER-2 aircraft, AVIRIS measures upwelling radiance in 224 contiguous channels between 400 and 2400 nm with a 10 nm spectral resolution (Vane et al., 1988). In October 2001, hemlock decline information was collected at 13 HWA monitoring plots (20×20 m). The end of the growing season was selected for sampling to facilitate the quantification of HWA infestation levels nearest the insect's maturity. No significant external events (e.g. drought, insect outbreak, etc) occurred between the time of the flight and ground truth sampling. To map hemlock abundance, percent hemlock basal area was recorded at 70 conifer dominated prism plots across the Catskills (Fig. 3). Geographic location was collected for all plots using a WAAS enabled Merridian Gold global positioning system (Rees, 2001).

Between the sensor and the surface, there is an extremely dynamic atmosphere that can dramatically alter the spectral radiation reflected from the canopy (Schowengerdt, 1997). In order to account for absorption and scattering by gasses and particulates as light passes through the atmosphere, atmospheric calibration algorithms using radiative transfer codes, rescale raw radiance data to surface reflectance by correcting for atmospheric influence (Van der Meer & de Jong, 2001). Atmospheric Correction Now software (ACORN 4.0 Analytical Imaging and Geophysics LLC, ImSpec 2002), developed specifically for hyperspectral sensors such as AVIRIS, removed atmospheric effects in the data using averaged time and geographic inputs from the five individual AVIRIS runs.

With a field of view of 30°, AVIRIS samples with view zenith angles of up to 15° to each side of nadir. This causes

a nearly linear decrease in reflectance as the view angle moves from forelit to backlit surfaces (Kennedy et al., 1997). To remove the resulting view-angle brightness gradient while maintaining the radiometric integrity of the image, the AVIRIS imagery was corrected using a CSIRO destreak algorithm (Datt et al., 2003), modified by the authors to employ global statistics averaged from all 5 runs. This linear algorithm normalized the mean and standard deviation of each column to the global mean and variance for each wavelength in the full image (Datt et al., 2003).

After atmospheric and brightness corrections, the imagery was geometrically registered to a USGS 1 m resolution digital orthoquads using a polynomial degree 2 warping method (ENVI 4.0 software, Research Systems, Inc). Each of the five runs were registered individually before mosaicing, with an average of 325 ground control points used per run and resulting in an average control point total error of 3.85 m. AVIRIS reflectance spectra were then extracted for pixels covering each of the 13 decline and 70 abundance plots (Fig. 1).

2.2. Hemlock abundance

Seventy field plots were randomly selected from primarily evergreen dominated areas within the AVIRIS imagery to determine the percent hemlock basal area using a basal area factor 10 prism. Mixture Tuned Matched Filtering (MTMF), (Nielsen, 2001; Tompkins et al., 1997; Williams & Hunt, 2002) was used to quantify the hemlock component of each pixel. This involved first reducing the 224-band AVIRIS image to a 28-band Minimum Noise Fraction (MNF) transformed image. This MNF transform as modified from Green et al. (1988) and implemented in ENVI, is essentially two cascaded Principal Components transformations which removes noise and reduces dimensionality in the data. Transformed spectra from 7 “pure hemlock” calibration pixels with greater than 90% hemlock cover were then used to calibrate the MTMF. Output from the MTMF included probability and infeasibility data for each pixel. A linear regression based on probability and infeasibility data was constructed from the 70 prism plots to predict percent hemlock. This equation was then applied to the MTMF output for calculation of percent hemlock basal on a pixel-by-pixel basis.

2.3. Hemlock decline

The five canopy dominant hemlocks on the 13 established monitoring plots were assessed using methods specifically designed to quantify the various sequential symptoms of decline that follow adelgid infestation. This included the percent of terminal branchlets with new growth (R. Evans personal communication), percent transparency (quantified using a concave spherical densiometer (Pontius et al., 2002)), percent fine twig dieback, and live crown ratio (USDA Forest Service Crown Rating Guide). Repeatability across a subset of plots was tested using five different field crews. There were no significant differences in decline measurements between crews, ensuring the consistency of our measurements. The categories of hemlock health described in Table 1 reflect the typical characteristics for each health measurement at various categories of hemlock decline. Health category assignments for each measurement on a tree were averaged to determine one overall decline rating that best described tree health (where 0=perfect health, 10=dead). Health scores were averaged for the five canopy dominant trees on each plot to determine a continuous plot level health rating for comparison to hyperspectral imagery. Visual symptoms are not apparent in the field until decline class 3 when transparency and dieback reach 15% and 5% respectively.

Existing decline detecting indices (Table 2) were calculated for each plot and entered into a stepwise linear regression, along with a suite of individual wavelengths significantly correlated with hemlock decline in a previous ASD FieldSpec Pro benchtop study (Pontius et al., 2005).

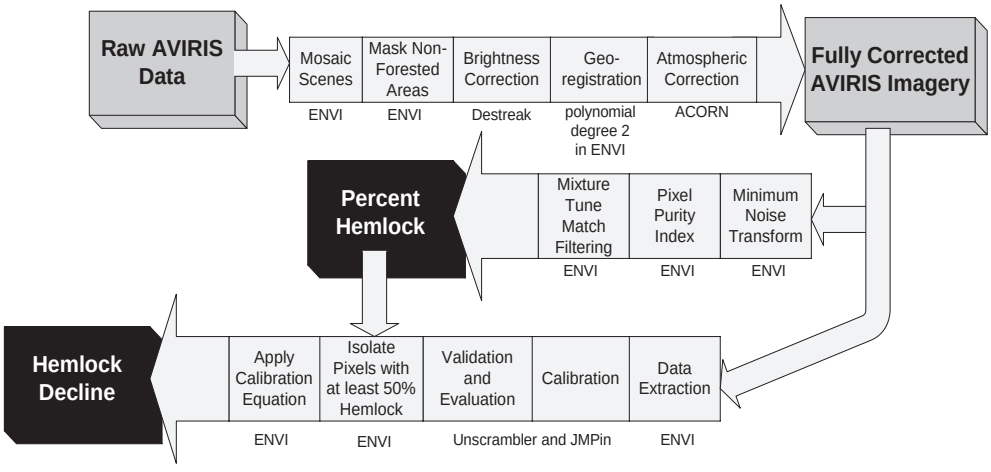

Fig. 1. The steps involved in processing the raw AVIRIS imagery and then creating the hemlock abundance and decline coverages over the Catskills.

Table 1
Decline rating summary: the best-fit categories for each of the individual measurements were averaged to determine which decline rating best described each tree's overall health

Decline class	Health status	Typical characteristics
0	Perfect health	All branchlets produce a flush of new growth Minimal canopy transparency No fine twig dieback More than 90% of the total tree height is photosynthethically active
1	Very healthy	Almost all branchlets produce new growth Only 6% to 9% of the canopy is transparent Fine twig dieback is minimal 80% to 89% of canopy is photosynthetically active
2	Healthy (typical healthy forest co-dominant)	Over 85% of terminal branchlets produce new growth 10% to 14% canopy transparency Less than 5% fine twig dieback 70% to 79% of canopy is photosynthetically active
3	Earliest decline	Slight reductions in new growth production (80% to 84%) 15% to 19% canopy transparency 5% to 10% fine twig dieback 65% to 69% of canopy is photosynthetically active
4	Light decline	More noticeable reductions in new growth (70% to 74%) 20% to 24% canopy transparency Approaching 10% fine twig dieback 60% to 64% of canopy is photosynthetically active
5	Light to moderate decline	Less than 3/4 of branchlets are producing more growth (70% to 74%) 25% to 29% canopy transparency 10% to 15% fine twig dieback 50% to 59% of canopy is photosynthetically active
6	Moderate decline	Only 60% to 69% of terminals produce a flush of new growth 30% to 34% canopy transparency Up to 15% fine twig dieback 40% to 49% of canopy is photosynthetically active
7	Moderate to severe decline	Barely half (40% to 59%) of terminals produce a flush of new growth 35 to 39% of the canopy is transparent 15 to 20% fine twig dieback 30% to 39% of canopy is photosynthetically active
8	Severe decline	Barely 1/3 (20% to 39%) of terminals produce a flush of new growth 40% to 44% of the canopy is transparent Up to 20% fine twig dieback 20% to 29% of canopy is photosynthetically active
9	Near death	Less than 20% of terminals produce a flush of new growth More than 45% of canopy is transparent Greater than 25% fine twig dieback Less than 20% of the canopy is photosynthetically active
10	Dead	100% defoliated

Visual symptoms are not apparent in the field until decline class 3 when transparency and dieback reach 15% and 5 % respectively.

Due to the small sample size, a maximum of 2 terms and conservative significance cutoff limits were established for each of the regression steps to avoid over fitting (probability to enter = 0.250, probability to leave = 0.01). Mallow's Cp and PRESS statistics were used to compare the predictive abilities of various models (Kozak & Kozak, 2003). Because of the small sample size, full double-cross validation (jackknifed residuals) was used in lieu of independent validation to assess predictive abilities (Kozak & Kozak, 2003). After establishing the best-fit hemlock decline model, the resulting equation was applied to all pixels with greater than 40% hemlock basal area on a pixel-by-pixel basis.

3. Results and discussion

3.1. Hemlock abundance

Percent hemlock basal area ranged from 0% to 100% on the 70 abundance plots, with an average of 49% (Table 3). Of these plots, the majority were dominated by evergreen species, with only 13% classified as hardwood mix or non-forested types. Because of the domination of evergreen stands in this data set, this becomes a strong test of how well hemlock can be differentiated from other spectrally similar conifer species.

Output from the MTMF included a) the probability that the pure hemlock signature was a component of reflectance and b) the infeasibility of the pure hemlock signature as a component of reflectance for each pixel. These 2 variables were input into Eq. (1) to calibrate percent hemlock basal area across the 70 prism plots. This translation of MTMF data to abundance reported an R^2 of 0.65 and a RMSE of 12 (Fig. 2). For comparison to straight classifications of dominant cover type, the MTMF based regression was able to correctly differentiate hemlock/non-hemlock (cutoff at 40% hemlock basal area) stands 83% of the time.

$$\text{Abundance} = 76.10 + (\text{Prob}*41.18) - (\text{Infeas}*5.53). \quad (1)$$

The linear regression equation to predict percent hemlock basal area where Prob = the probability output and Infeas =

Table 2
Known decline related indices: a list of existing indices included in our analyses that are known to have strong relationships with decline specific physiological responses (i.e. reductions in photosynthesis or chlorophyll content), where R = reflectance and FD = first derivative

Index	Formula	Primary absorbance feature	Citation
Carter and Miller Stress	$\mathrm{CMS} = \frac{R694\,\mathrm{nm}}{R760\,\mathrm{nm}}$	Chlorophyll content	(Carter & Miller, 1994)
Curvature index	$\mathrm{CI} = \frac{R683\,\mathrm{nm}*2}{R675\,\mathrm{nm}*R691\,\mathrm{nm}}$		(Zarco-Tejada et al., 2002)
Derivative chlorophyll index	$\mathrm{DCI} = \frac{\mathrm{FD705\,nm}}{\mathrm{FD723\,nm}}$	Chlorophyll a and b content	(Zarco-Tejada et al., 2002)
Chlorophyll fluorescence	$CF = \frac{FD690\,\mathrm{nm}}{FD735\mathrm{nm}}$		(Mohammed et al., 1995)
Normalized difference vegetation index	$\mathrm{NDVI} = \frac{R800\ \mathrm{nm} - R680\ \mathrm{nm}}{R800\ \mathrm{nm}*R680\ \mathrm{nm}}$	Chlorophyll content and energy absorption	(Deblonde & Cihlar, 1993; Gamon et al., 1997; Myneni et al., 1995; Rouse et al., 1974)
Photo-chemical reflectance index	$\mathrm{PRI} = \frac{R531\ \mathrm{nm} - R570\ \mathrm{nm}}{R531\ \mathrm{nm}*R570\ \mathrm{nm}}$		(Gamon et al., 1990, 1997; Rahman et al., 2001)
Red edge inflection point	$\mathrm{REIP} = \lambda FD\ \max$	Chlorophyll a content; green vegetation density	(Gitelson & Merzlyak, 1996; Rock et al., 1988; Vogelmann et al., 1993)
Ratio vegetation index	$\mathrm{RVI} = \frac{R800\ \mathrm{nm}}{R680\ \mathrm{nm}}$	Chlorophyll content	(Pearson & Miller, 1972; Royle & Lathrop, 2002)
Water band index	$\mathrm{WBI} = \frac{R970\ \mathrm{nm}}{R900\ \mathrm{nm}}$	Canopy water content	(Carter, 1993; Penuelas et al., 1997; Tucker, 1980)

the infeasibility output from a MTMF process. Validation statistics were: $R^2 = 0.65$ and RMSE = 12.

Much of the error introduced in this model resulted from pine-dominated stands predicted to have a higher percentage of hemlock than was actually present (Fig. 2). The spectral unmixing methods appear to be able to identify all mature, dominant hemlock stands accurately. However, there is also the risk of classifying dense, white pine stands as containing some hemlock when they do not. The most erroneous prism plots used in this validation include red pine plantation stands surrounded by mixed hemlock forest. It is our belief that this problem may not be so much a limitation of the AVIRIS instrument as a georegistration issue. If registration

Table 3
Plot demographics: of the 70 basal area prism points used to validate the MTMF for hemlock abundance, the vast majority were dominated by evergreen species

Type	N	Avg. % HE	Min % HE	Max % HE
Field	3	0	0	0
Hemlock hardwood mix	26	54	0	48
Hemlock	21	86	50	100
Larch	1	0	0	0
Red spruce mix	4	48	0	11
White/red pine	15	2	0	30
	70	49	0	100

These points cover a range from 0% to 100% hemlock with an average of 49% hemlock basal area.

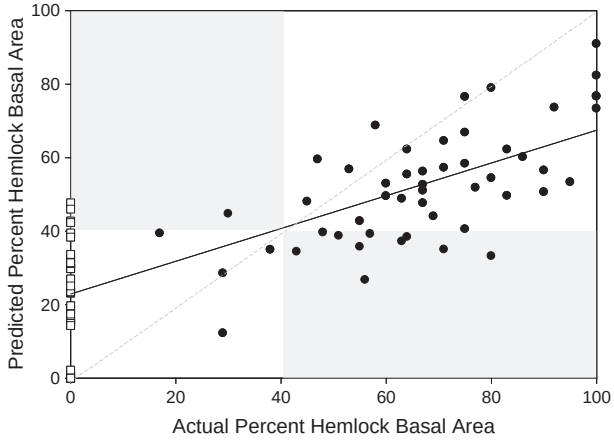

Fig. 2. Hemlock abundance was predicted with an R^2 of 0.65 and RMSE of 12. Most error was manifest as under predicting stands with significant understory hemlock (bottom right gray) and pine dominated stands predicted to have hemlock (upper left gray). Circles represent hemlock and mixed hemlock stands, open squares are dominated by other evergreen species. Hemlock dominated stands were differentiated from non-hemlock stands with 83% accuracy.

is off by several meters around these pine plantation stands, the extracted spectra for accuracy assessment may indeed contain a component of hemlock. While this error is significant in our abundance predictions, we believe that this equation adequately identifies hemlock dominated stands for the application of decline predictions in this study.

In the upper end of the range, hemlock abundance predictions were often low (Fig. 2). This may be due to the inclusion of understory hemlock in the prism plot percent basal area measurements that are not visible to the AVIRIS sensor. In mixed, mid-successional stands, hemlock may not be mature and present in the canopy in numbers sufficient to impact canopy spectral signatures. Such trees are likely shaded out by the intermediate successional, mature hardwood or pine canopy dominants. Mickelson et al. (1998) found similar problems with mixed hemlock stands using multi-temporal Landsat TM data.

For problems such as the HWA induced hemlock decline, it is useful to map actual hemlock abundance so that areas of relative susceptibility and ecological impact can be identified. Applying Eq. (1) to the full AVIRIS image (Fig. 3) highlights the heavy concentration of hemlock in riparian areas. This suggests that widespread hemlock decline and mortality could be a significant factor in deteriorating surface water quality in the Catskills.

3.2. Hemlock decline

While multiple factors were significantly correlated with decline (Table 4), a mixed, stepwise linear regression suggests that only R683 and the Water Band Index (WBI) (Carter, 1993; Penuelas et al., 1997; Tucker, 1980) were necessary to predict decline across the low to mid range of decline (R^2=0.88, RMSE=0.23 and a PRESS=1.67) (Eq. (2); Fig. 4). Treated as a class variable by rounding to the nearest integer, this predicted decline class on the calibration data with 85% accuracy and to within one class with 100% accuracy. An average jackknifed residual error of 0.13 indicates the expected accuracy on an independent data set would also be good across the range of data. These wavelengths were also significantly correlated with decline (WBI r=0.53, $R683$ r=0.28) in a previous leaf-level study (Pontius et al., 2005). The full spectrum with key wavelengths highlighted can be seen in Fig. 5.

$$\text{Decline} = -16.82 + (R683*0.02) + (\text{WBI}*15.40). \quad (2)$$

The linear regression equation to predict hemlock decline where R683 = the reflectance at 683 nm and WBI = the Water Band Index as defined in Table 2. Validation statistics were: R2 = 0.88, RMSE = 0.23 and PRESS = 1.67.

Given that Eq. (2) works well on an empirical basis, it is useful to understand whether the wavelengths and indices used in the regression equations are theoretically related to tree health or physiological function. The strongest correlation with decline, and one of the key terms in Eq. (2), occurred at R683 nm. This wavelength is associated with chlorophyll a absorbance (Carter, 1993; Carter & Knapp, 2001; Kolling et al., 1996; Zarco-Tejada et al., 2002).

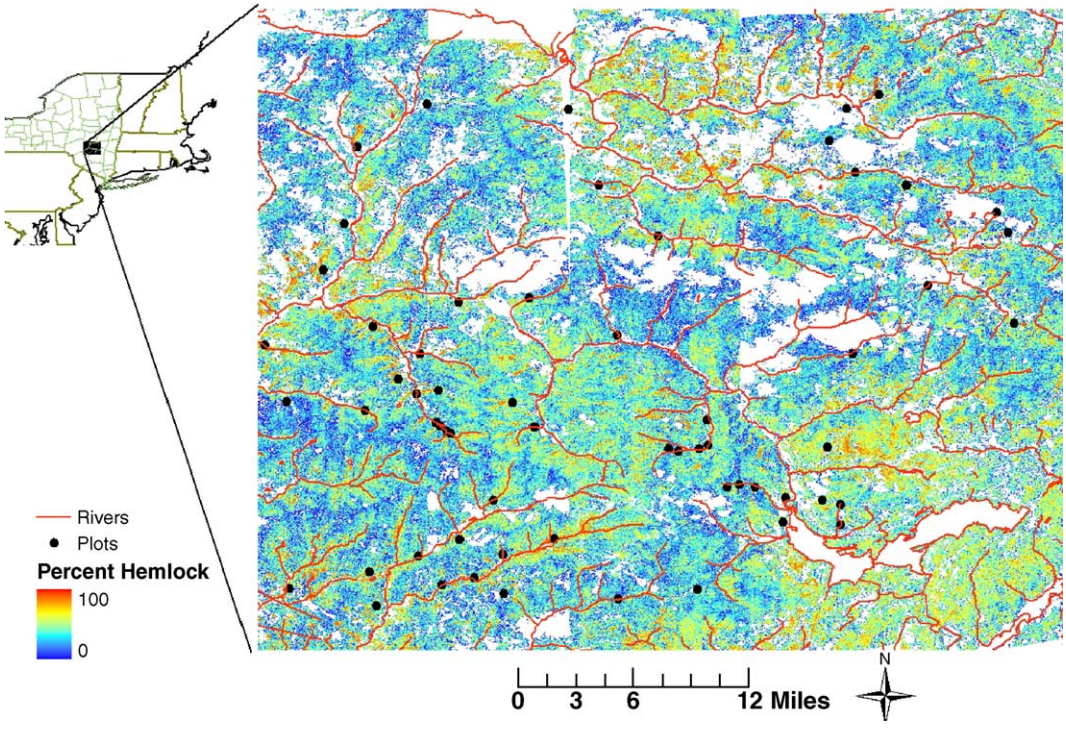

Fig. 3. A map of percent hemlock basal area highlights the high concentration of hemlock in lowland and riparian areas.

Table 4
Pairwise correlations with decline are reported with their known absorbance features

Wavelength	Correlation with decline	Absorbance feature	Citation
$R683$	**0.8542**	Chlorophyll a	(Carter, 1993)
$R1653$	**0.6508**	Benzene rings, C–H stretch	(Williams & Norris, 2001)
$R952$	**0.4611**	Water	(Williams & Norris, 2001)
$R760$	**0.4347**	Water	(Osborne & Fearn, 1986)
$CF = \frac{FD690\ nm}{FD735\ nm}$	**0.3992**	Chlorophyll florescence; photosynthetic activity	(Mohammed et al., 1995)
$WBI = \frac{R970\ nm}{R900\ nm}$	**0.3787**	Canopy water content	(Carter, 1993; Penuelas et al., 1997; Tucker, 1980)
$RVI = \frac{R800\ nm}{R680\ nm}$	−0.3582	Chlorophyll content	(Pearson & Miller, 1972; Royle & Lathrop, 2002)
$PRI = \frac{R531\ nm - R570\ nm}{R531\ nm + R570\ nm}$	0.3578	Xanthohyll cycle activity	(Gamon et al., 1990, 1997; Rahman et al., 2001)
$CMS = \frac{R694\ nm}{R760\ nm}$	0.3026	Chlorophyll content	(Carter & Miller, 1994)
$REIP = \lambda FD\ max$	0.2997	Chlorophyll a content; green vegetation density	(Gitelson et al., 1996; Rock et al., 1988; Vogelmann et al., 1993)
$NDVI = \frac{R800\ nm - R680\ nm}{R800\ nm + R680\ nm}$	−0.2717	Chlorophyll content and energy absorption	(Deblonde & Cihlar, 1993; Gamon et al., 1997)
$CI = \frac{R683\ nm*2}{R675\ nm*R691\ nm}$	0.1254	Chlorophyll florescence	(Zarco-Tejada et al., 2002)
$DCI = \frac{FD705\ nm}{FD723\ nm}$	−0.0523	Chlorophyll a and b content; chlorophyll florescence	(Zarco-Tejada et al., 2002)

Bold indicates significance at the $p<0.2$ level. Variables are listed by correlation strength. Only $R683$ nm and the WBI were retained for inclusion in the stepwise linear regression to predict decline.

Chlorophyll content is a good detector of stress because of its direct role in photosynthesis. Increasing reflectance near the 700 nm range represents the often-reported blue shift in stressed plants. This shift in the red edge inflection point results from stress induced reductions in chlorophyll content (Cibula & Carter, 1992; Rock et al., 1988). Because the absorptivity of chlorophyll is relatively low in this region, even small decreases in chlorophyll content result in significantly decreased absorption and increased reflectance in stressed plants (Carter, 1993; Carter & Knapp, 2001). Stress induced changes in reflectance have been directly linked to foliar chlorophyll content in numerous studies (Gitelson & Merzlyak, 1996; Rock et al., 1988; Vogelmann et al., 1993).

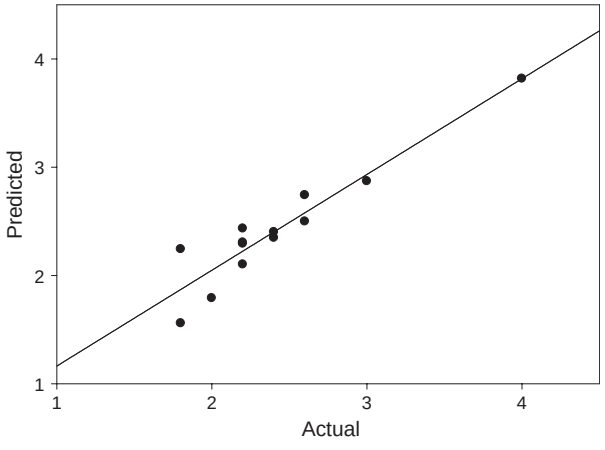

Fig. 4. The two-term linear regression equation based on $R683$ nm and the WBI predicted hemlock decline with an R^2 of 0.88 and RMSE of 0.23.

The WBI was the second key term in predicting hemlock decline. This index is a ratio between the reflectance at 970 nm, where absorbance by water is evident, and 900 nm used as a reference, “control” band. Several studies have shown that the WBI closely tracks changes in leaf relative water content, leaf water potential and stomatal conductance (Bull, 1991; Penuelas et al., 1993; Penuelas et al., 1996, 1994). In some species, WBI was able to track even mild water stress (Penuelas et al., 1996).

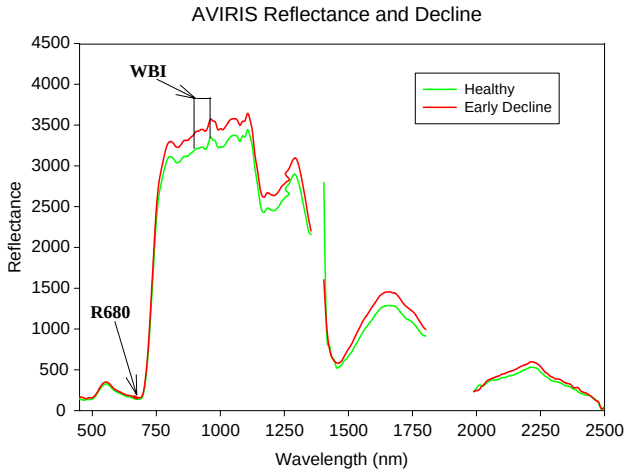

Fig. 5. AVIRIS data extends from 450 to 2500 nm with strong atmospheric water absorption bands removed and reflectance averaged for healthy samples (Decline<2) and those experiencing the early stages of decline (2<Decline<4). We highlight those wavelengths found to be significant in predicting hemlock decline.

Relative susceptibility of hemlock to HWA has been linked to various site and landscape factors related to water availability (Bonneau et al., 1997; Onken, 1995; Royle & Lathrop, 1999). Drier conditions stress already weakened tress, making them more susceptible to HWA and decline. There is also evidence that HWA injects toxic saliva at feeding sites (McClure et al., 1996). It is postulated that the toxic effects of this saliva may include a constricting effect on xylem, which could lead to leaf dehydration following infestation (Shields et al., 1995). Although we did not directly measure leaf water content, it is plausible that trees experiencing decline may be under some form of water stress.

The predictive decline equation (Eq. (2)) was created using spectra from hemlock-dominated stands (40% to 100% hemlock). Therefore, we only predicted hemlock decline for all pixels in the AVIRIS imagery with greater than 40% hemlock as predicted by Eq. (1). Predicted hemlock decline ranged from 0 to 7.7 across the Catskills as compared to 1.8 to 4.1 found on the original 13 calibration plots (Fig. 6).

Ideally, calibration equations are developed with field data covering the full range of possible conditions (Martin & Aber, 1997). Because HWA infestation was still relatively new to the Catskills in 2001, severely declining trees were difficult to find. To test the linear relationship between the predictive equation and decline beyond the range of input calibration data, the equation was applied to a 100 sample, tree level dataset from a benchtop spectrometer based on methods described in Pontius et al. (2005). Eq. (2) predicted tree level decline across the complete range with a one-class tolerance accuracy of 82%. Therefore, we believe that this equation is linear and should hold beyond the range of decline available for calibration development.

More severe decline is evident in the southeastern region of the imagery (Fig. 6), coinciding with the area first infested by HWA (Montgomery personal communication). Average jackknifed residuals of 0.13 indicate that this equation should also work on independent data from the

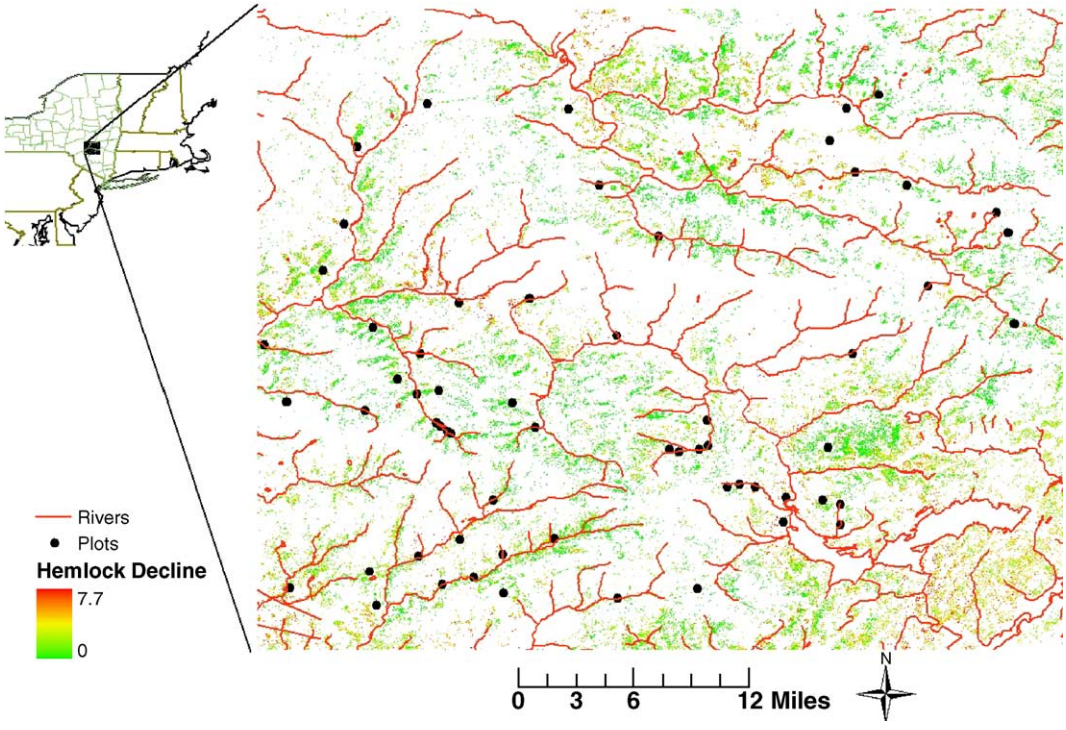

Fig. 6. Applied to all pixels with greater than 40% hemlock basal area, the decline prediction highlights more severe decline symptoms in the southeastern corner of the region where HWA has the longest history in hemlock stands. Other stressors are not excluded from this analysis.

same range (Kozak & Kozak, 2003). Additional data from 8 New York State Department of Environmental Conservation (DEC) hemlock-monitoring plots were examined as a preliminary independent validation. While the DEC decline assessment was limited to a coarse evaluation of overall hemlock health (categorized as healthy, HWA present but no visible damage, or discoloration), their assessments were predicted with a one-class tolerance accuracy of 88% (labeling healthy as decline class 2, HWA present but no visible damage as decline class 3 and discoloration as decline class 4). While these results are promising, a more rigorous validation covering the range of decline symptoms in the Catskills and matching our assessment methods is required to adequately represent the full range of conditions expected in natural hemlock stands.

HWA damage differs from many other forest stressors in that there is little noticeable change in color of damaged foliage (Royle & Lathrop, 2002). Damage primarily appears as a gradual thinning of the foliage with tree death occurring in 4 to 6 years (McClure, 1987). Defoliation does not reach levels classified as the very first stage of defoliation (>5% dieback or >15% transparency) by traditional field-based methods until after health class 3. Because Eq. (2) works well below class 3, it appears that such imagery has the capability to identify decline pre-visual symptoms.

In order for this technology to be applicable on a large spatial and temporal scale, the relationships presented here must also be shown to work on other datasets. Because the AVIRIS data collected over the Catskills covered 5 different flight lines, we believe that the relationships presented here will prove robust enough for application to other hyperspectral imagery. Further, because the initial selection of wavelengths for examination with the AVIRIS imagery was based on results from a previous ASD benchtop spectrometer, in which both studies showed similar relationships for key wavelengths and indices (Pontius et al., 2005), we believe that these relationships will also hold across other hyperspectral instruments.

There is little evidence that these technologies can diagnose causal agents, as decline may be related to a variety of factors. Still, the best hope of successful biological control for HWA must target newly infested areas where trees are still relatively healthy. Therefore, the ability to identify stands early is essential to the development of sound forest management strategies.

4. Conclusions

This work indicated that hyperspectral sensors have the ability to assess detailed hemlock decline on a landscape scale. By training on pure hemlock spectra and running a MTMF on the full AVIRIS spectrum, hemlock dominated stands were identified with 83% accuracy. The full spectrum was not required to predict hemlock decline. Using a linear regression equation based on one chlorophyll ($R$683 nm) and one canopy water content (WBI) sensitive variable, early decline was predicted with $R^2=0.88$ and average jackknifed residual error=0.13. These variables capture the physiological changes (reductions in chlorophyll content and needle desiccation) expected to accompany early hemlock decline. The accuracy of the predictions below decline rating 3, when visual symptoms are first apparent in the field, indicates that these wavelengths may be capable of assessing pre-visual decline symptoms.

Although this technique is not diagnostic, it is likely that most declining hemlock in this region is impacted by HWA. More research is currently underway to assess the applicability of this equation to other sensors and across areas with a greater range of hemlock health. We anticipate that the ability to map hemlock and monitor decline across the landscape, will prove essential to the ultimate management and control of invasives such as HWA.

Acknowledgements

This work would not have been possible without generous funding from the USDA Forest Service Scientific Recruitment Initiative and the Science and Technology Development Program. Acquisition and processing of remote sensing imagery has also been funded in part by NASA and the United States Environmental Protection Agency through grant #R825865 to the University of New Hampshire. For help in the field and lab, we wish to thank: Lucie Plourde, Collin Pinney, Shannon Cromley, Anne Gorham, Melissa Sytek, Jeremy Fontenault, Mike Gagnon, Jamie Lavigne, Garrett Dubois and John Richardson. The support of the following organizations, researchers and land managers was also key in locating and accessing appropriate study plots: NY State Department of Environmental Conservation, NY State Park System, and the USDA Forest Service Northeastern Research Station.

References

Baret, F., & Guyot, G. (1991). Potentials and limits of vegetation indexes for LAI and APAR assessment. *Remote Sensing of Environment*, *35*, 161–173.

Bonneau, L. R., ODell, T. C. D. L., Broderick, S. H., & Sheilds, K. S. (1997). *The impact of hemlock woolly adelgid on the health of eastern hemlock: An update from Connecticut*. University of Connecticut Cooperative Extension System.

Bull, C. R. (1991). Wavelength selection for near-infrared reflectance moisture meters. *Journal of Agricultural Engineering Research*, *49*, 113–125.

Carter, G. A. (1993). Responses of leaf spectral reflectance to plant stress. *American Journal of Botany*, *80*, 239–243.

Carter, G. A., & Knapp, A. K. (2001). Leaf optical properties in higher plants: Linking spectral characteristics to stress and chlorophyll concentration. *American Journal of Botany*, *88*, 677–684.

Carter, G. A., & Miller, R. L. (1994). Early detection of plant stress by digital imaging within narrow stress-sensitive wavebands. *Remote Sensing of Environment*, *50*, 295–302.

Castello, J. D., Leopold, D. J., & Smallidge, P. J. (1995). Pathogens, patterns and processes in forest ecosystems. *Bioscience*, *45*, 16–24.

Cibula, W. G., & Carter, G. A. (1992). Identification of a far red reflectance response to ectomycorrhizae in slash pine. *International Journal of Remote Sensing*, *13*, 925–932.

Datt, B., McVicar, T. R., Van Niel, T. G., Jupp, D. L. B., & Pearlman, J. S. (2003). Preprocessing EO-1 hyperion hyperspectral data to support the application of agricultural indexes. *IEEE Transactions on Geoscience and Remote Sensing*, *41*, 1246–1259.

Deblonde, G., & Cihlar, J. (1993). A multiyear analysis of the relationship between surface environmental variables and NDVI over the Canadian landmass. *Remote Sensing Reviews*, *7*, 151–177.

Gamon, J. A., Field, C. B., Bilger, W., Bjorkman, O., Fredeen, A. L., & Penuelas, J. (1990). Remote-sensing of the xanthophyll cycle and chlorophyll fluorescence in sunflower leaves and canopies. *Oecologia*, *85*, 1–7.

Gamon, J. A., Serrano, L., & Surfus, J. S. (1997). The photochemical reflectance index: An optical indicator of photosynthetic radiation use efficiency across species, functional types, and nutrient levels. *Oecologia*, *112*, 492–501.

Gitelson, A. A., & Merzlyak, M. N. (1996). Signature analysis of leaf reflectance spectra: Algorithm development of remote sensing of chlorophyll. *Journal of Plant Physiology*, *148*, 494–500.

Green, A. A., Berman, M., Switzer, P., & Craig, M. D. (1988). A transform for ordering multispectral data in terms of image quality with implications for noise removal. *IEEE Transactions on Geoscience and Remote Sensing*, *26*, 65–74.

Hoque, E., Hutzler, P. J. S., & Hiendl, H. (1990). Studies on reflective features of Norway spruce and their possible applications in remote-sensing of forest damage. *Toxicological and Environmental Chemistry*, *27*, 209–215.

Hoque, E., Hutzler, P. J. S., & Hiendl, H. (1992). Reflectance, color, and histological features as parameters for the early assessment of forest damages. *Canadian Journal of Remote Sensing*, *18*, 104–110.

Kennedy, R. E., Cohen, W. B., & Takao, G. (1997). Empirical methods to compensate for a view-angle-dependent brightness gradient in AVIRIS imagery. *Remote Sensing of Environment*, *62*, 277–291.

Kolling, C., Hoffmann, M., & Gulder, H. J. (1996). Soil chemistry depth gradients as characteristic state variables of forest ecosystems. *Zeitschrift Fur Pflanzenernahrung Und Bodenkunde*, *159*, 69–77.

Kozak, A., & Kozak, R. (2003). Does cross validation provide additional information in the evaluation of regression models? *Canadian Journal of Forest Research*, *33*, 976–987.

Lambert, N. J., Ardo, J., Rock, B. N., & Vogelmann, J. E. (1995). Spectral characterization and regression-based classification of forest damage in Norway spruce stands in the Czech-Republic using Landsat Thematic Mapper data. *International Journal of Remote Sensing*, *16*, 1261–1287.

Liebhold, A. M., McDonald, W. L., Bergdahl, D., & Mastro, V. S. (1995). Invasion by exotic forest pests: A threat to forest ecosystems. *Forest Science Mongraphs*, *30*, 1–49.

Martin, M. E., & Aber, J. A. (1997). High spectral resolution remote sensing of forest canopy lignin, nitrogen, and ecosystem processes. *Ecological Applications*, *7*, 431–443.

McClure, M. S. (1987). *Biology and control of hemlock woolly adelgid*. CT: Connecticut Agricultural Experiment Station.

McClure, M. S. (1991). Nitrogen fertilization of hemlock increases susceptibility to hemlock woolly adelgid. *Journal of Arboriculture*, *17*, 227–229.

McClure, M. S. (1995). Biology of *Adelges tsugae* and its potential for spread in the northeastern United States. *Proceedings of the First Hemlock Woolly Adelgid Review, Charlottesville, VA* (pp. 16–24).

McClure, M. S., Salom, S. M., & Shields, K. S. (1996). *Hemlock woolly adelgid*. Morgantown, WV: Forest Health Technology Enterprise Team, USDA Forest Service.

Mickelson, J. G., Civco, D. L., & Silander, J. A. (1998). Delineating forest canopy species in the northeastern United States using multi-temporal TM imagery. *Photogrammetric Engineering and Remote Sensing*, *64*, 891–904.

Mohammed, G. H., Binder, W. D., & Gillies, S. L. (1995). Chlorophyll fluorescence — a review of its practical forestry applications and instrumentation. *Scandinavian Journal of Forest Research*, *10*, 383–410.

Myneni, R. B., Hall, F. G., Sellers, P. J., & Marshak, A. L. (1995). The interpretation of spectral vegetation indexes. *IEEE Transactions on Geoscience and Remote Sensing*, *33*, 481–486.

Nielsen, A. A. (2001). Spectral mixture analysis: Linear and semi-parametric full and iterated partial unmixing in multi-and hyper-spectral image data. *Journal of Mathematical Imaging and Vision*, *15*, 17–37.

Onken, B. P. (1995). Long-term impact assessment of eastern hemlock forests. *Proceedings of the First Hemlock Woolly Adelgid Review, Charlottesville, VA* (pp. 58–63).

Orwig, D. A., & Foster, D. R. (1998). Forest response to the introduced hemlock woolly adelgid in southern New England, USA. *Journal of the Torrey Botanical Society*, *125*, 60–73.

Osborne, B. G., & Fearn, T. (1986). *Near-infrared spectroscopy in food analysis*. New York: John Wiley and Sons Inc.

Pearson, L., & Miller, L. D. (1972). Remote mapping of standing crop biomass for estimation of the productivity of the short-grass prairie, pawnee national grasslands, Colorado. *Proceedings of the 8th International Symposium on Remote Sensing of the Environment* (pp. 1357–1381).

Penuelas, J., Filella, I., Biel, C., Serrano, L., & Save, R. (1993). The reflectance at the 950–970 nm region as an indicator of plant water status. *International Journal of Remote Sensing*, *14*, 1887–1905.

Penuelas, J., Filella, I., Serrano, L., & Save, R. (1996). Cell wall elasticity and water index ($R$970 nm $R$900 nm) in wheat under different nitrogen availabilities. *International Journal of Remote Sensing*, *17*, 373–382.

Penuelas, J., Gamon, J., Freeden, A., Merino, J., & Field, C. (1994). Reflectance indices associated with physiological changes in nitrogen and water limited sunflower leaves. *Remote Sensing of Environment*, *48*, 135–146.

Penuelas, J., Pinol, J., Ogaya, R., & Filella, I. (1997). Estimation of plant water concentration by the reflectance water index WI ($R$900/$R$970). *International Journal of Remote Sensing*, *18*, 2869–2875.

Pinty, B., Leprieur, C., & Verstraete, M. M. (1993). Towards a quantitative interpretation of vegetation indices: Part I. Biophysical canopy properties and classical indices. *Remote Sensing Reviews*, *7*, 127–150.

Pontius, J., Hallett, R., & Martin, M. (2002). Examining the role of foliar chemistry in hemlock woolly adelgid infestation and hemlock decline. *Proceedings: Hemlock Woolly Adelgid in the Eastern United States Symposium, East Brunswick, NJ* (pp. 86–99).

Pontius, J., Hallett, R. A., & Martin, M. E. (2005). Assessing hemlock decline using hyperspectral imagery: Signature analysis, indices comparison and algorithm development. *Journal of Applied Spectroscopy*, *72*.

Rahman, A. F., Gamon, J. A., Fuentes, D. A., Roberts, D. A., & Prentiss, D. (2001). Modeling spatially distributed ecosystem flux of boreal forest using hyperspectral indices from AVIRIS imagery. *Journal of Geophysical Research-Atmospheres*, *106*, 33579–33591.

Rees, W. G. (2001). Improving the accuracy of low-cost GPS measurements for remote sensing applications. *International Journal of Remote Sensing*, *22*, 871–881.

Rock, B. N., Hoshizaki, T., & Miller, J. R. (1988). Comparison of insitu and airborne spectral measurements of the blue shift associated with forest decline. *Remote Sensing of Environment*, *24*, 109–127.

Rosengren, M., & Ekstrand, S. (1988). A method aiming at monitoring of large-area forest decline using satellite imagery. *Proceedings Seminar on Remote Sensing of Forest Decline Attributed to Air Pollution, Laxenburg, Austria* (pp. 2:1–2:20). Greenbelt, MD: International Institute for Applied Systems Analysis.

Rouse, J., Hass, R., Schell, J., Deering, D., & Harlan, J. (1974). *Monitoring the vernal advancement and retrogradation of natural vegetation*. Greenbelt, MD: NASA.

Royle, D., & Lathrop, R. (1999). The effects of site factors on the rate of hemlock decline: A case study in New Jersey. *Proceedings: Symposium on Sustainable Management of Hemlock Ecosystems in Eastern North America* (pp. 103–104).

Royle, D. D., & Lathrop, R. G. (1997). Monitoring hemlock forest health in New Jersey using Landsat TM Data and change detection techniques. *Forest Science*, *43*, 327–335.

Royle, D. D., & Lathrop, R. G. (2002). Discriminating *Tsuga canadensis* hemlock forest defoliation using remotely sensed change detection. *Journal of Nematology*, *34*, 213–221.

Royle, D. D., Lathrop Jr., R. G., & Koeck, G. P. (1995). Mapping hemlock decline in northern New Jersey using Landsat TM imagery. *Proceedings of the First Hemlock Woolly Adelgid Review, Charlottesville, VA* (pp. 75–86).

Sampson, P. H., Mohammed, G. H., Zarco-Tejada, P. J., Miller, J. R., Noland, T. L., Irving, D., et al. (2000). The bioindicators of forest condition project: A physiological, remote sensing approach. *Forestry Chronicle*, *76*, 941–952.

Schowengerdt, R. A. (1997). *Remote sensing, models and methods for image processing* (2nd ed.) San Diego, CA: Academic Press.

Shields, K. S., Young, R. F., & Berlyn, G. P. (1995). Hemlock woolly adelgid feeding mechanisms. *Proceedings of the First Hemlock Woolly Adelgid Review, Charlottesville, VA* (pp. 36–41).

Souto, D., Luther, T., & Chianese, B. (1995). Past and current status of HWA in eastern and Carolina hemlock stands. *Proceedings of the First Hemlock Woolly Adelgid Review, Charlottesville, VA* (pp. 9–15).

Tompkins, S., Mustard, J. F., Pieters, C. M., & Forsyth, D. W. (1997). Optimization of endmembers for spectral mixture analysis. *Remote Sensing of Environment*, *59*, 472–489.

Treitz, P. M., & Howarth, P. J. (1999). Hyperspectral remote sensing for estimating biophysical parameters of forest ecosystems. *Progress in Physical Geography*, *23*, 359–390.

Tucker, C. J. (1980). Remote sensing of leaf water content in the near infrared. *Remote Sensing of the Environment*, *10*, 23–32.

Van der Meer, F. D., & de Jong, S. M. (2001). Imaging spectroscopy. *Basic principals and prospective applications*. Boston, MA: Kluwer Academic Publishers.

Vane, G., Porter, W. M., Reimer, J. H., Chrien, T. C., & Green, R. O. (1988). AVIRIS performance during the 1987 flight season: An AVIRIS project assessment and summary of the NASA-sponsored performance evaluation. *Proceedings of the Airborne Visible/Infrared Imaging Spectrometer (AVIRIS) Performance Evaluation Workshop* (pp. 1–20).

Vogelmann, J. E., Rock, B. N., & Moss, D. M. (1993). Red edge spectral measurements from sugar maple leaves. *International Journal of Remote Sensing*, *14*, 1563–1575.

Williams, A. P., & Hunt, E. R. (2002). Estimation of leafy spurge cover from hyperspectral imagery using mixture tuned matched filtering. *Remote Sensing of Environment*, *82*, 446–456.

Williams, P., & Norris, K. (2001). *Near-infrared technology in the agricultural and food industries*. St. Paul, MN: American Association of Cereal Chemists.

Zarco-Tejada, P. J., Miller, J. R., Mohammed, G. H., Noland, T. L., & Sampson, P. H. (2000). Optical indices as bioindicators of forest condition from hyperspectral CASI data. *Symposium of the European Association of Remote Sensing Laboratories, Valladolid Spain* (pp. 517–522).

Zarco-Tejada, P. J., Miller, J. R., Mohammed, G. H., Noland, T. L., & Sampson, P. H. (2002). Vegetation stress detection through chlorophyll $_{a+b}$ estimation and fluorescence effects on hyperspectral imagery. *Journal of Environmental Quality*, *31*, 1433–1441.